The Astrophysical Journal, 664: L79–L82, 2007 August 1

SUZAKU OBSERVATIONS OF ACTIVE GALACTIC NUCLEI DETECTED IN THE *SWIFT* BAT SURVEY: DISCOVERY OF A "NEW TYPE" OF BURIED SUPERMASSIVE BLACK HOLES

Yoshihiro Ueda,[1] Satoshi Eguchi,[1] Yuichi Terashima,[2] Richard Mushotzky,[3] Jack Tueller,[3] Craig Markwardt,[3] Neil Gehrels,[3] Yasuhiro Hashimoto,[4] and Stephen Potter[4]

Received 2007 March 11; accepted 2007 June 1; published 2007 July 18

ABSTRACT

We present the *Suzaku* broadband observations of two AGNs detected by the *Swift* BAT hard X-ray (>15 keV) survey that did not have previous X-ray data, SWIFT J0601.9−8636 and SWIFT J0138.6−4001. The *Suzaku* spectra reveal in both objects a heavily absorbed power-law component with a column density of $N_{\rm H} \simeq 10^{23.5}$–$10^{24}$ cm^{-2} that dominates above 10 keV and an intense reflection component with a solid angle $\gtrsim 2\pi$ from a cold, optically thick medium. We find that these AGNs have an extremely small fraction of scattered light from the nucleus, $\lesssim 0.5\%$ with respect to the intrinsic power-law component. This indicates that they are buried in a very geometrically thick torus with a small opening angle and/or have an unusually small amount of gas responsible for scattering. In the former case, the geometry of SWIFT J0601.9−8636 should be nearly face-on as inferred from the small absorption for the reflection component. The discovery of two such objects in this small sample implies that there must be a significant number of yet unrecognized, very Compton thick AGNs viewed at larger inclination angles in the local universe, which are difficult to detect even in the currently most sensitive optical or hard X-ray surveys.

Subject headings: galaxies: active — gamma rays: observations — X-rays: galaxies — X-rays: general

Online material: color figure

1. INTRODUCTION

Many observations imply the presence of a large number of heavily obscured active galactic nuclei (AGNs) in the local universe (e.g., Maiolino et al. 1998; Risaliti et al. 1999). The number density of AGNs subject to absorption with a line-of-sight hydrogen column density $\log N_{\rm H} \gtrsim 23.5$ cm^{-2} is a key parameter in understanding the accretion history of the universe (e.g., Setti & Woltjer 1989; Fabian 1999). According to synthesis models of the X-ray background (XRB; e.g., Ueda et al. 2003; Gilli et al. 2007), much of the peak intensity of the XRB at 30 keV should be produced by these objects. In spite of the potential importance of their contribution to the growth of supermassive black holes (Marconi et al. 2004), the nature of this population of AGNs, even in the local universe, is only poorly understood due to strong biases against detecting them. In these objects, the direct emission in the UV, optical, and near-IR bands as well as at $E < 10$ keV from the nucleus is almost completely blocked by obscuring matter, making it difficult to probe the central engine.

Hard X-ray surveys at energies above 10–15 keV provide us with an ideal opportunity to select this population of AGNs as long as the column density is less than $\log N_{\rm H} \approx 24.5$ cm^{-2}. Recent surveys performed with the *Swift* Burst Alert Telescope (BAT; 15–200 keV; Markwardt et al. 2005) and *INTEGRAL* (10–100 keV; Bassani et al. 2006; Beckmann et al. 2006; Sazonov et al. 2007), because of their relative insensitivity to absorption, are providing one of the most unbiased AGN samples in the local universe including Compton thick AGNs, i.e., those with $\log N_{\rm H} > 24$ cm^{-2}. In fact, these surveys have started to detect hidden AGNs in the local universe located in galaxies that were previously unrecognized to contain an active nucleus at other wavelengths.

To unveil the nature of these new hard X-ray sources, follow-up observations covering a broad energy band are crucial. In this Letter, we present the first results from follow-up observations with the *Suzaku* observatory (Mitsuda et al. 2007) of the AGNs SWIFT J0601.9−8636 and SWIFT J0138.6−4001 detected in the *Swift* BAT survey. These targets are essentially randomly selected from a bright *Swift* AGN sample for which soft X-ray (<10 keV) spectroscopic observations had never been performed and are thus reasonable representatives of unknown AGN populations selected by hard X-rays above 15 keV. In § 3, we also present an optical spectrum of SWIFT J0601.9−8636 taken at the South African Astronomical Observatory (SAAO) 1.9 m telescope. The cosmological parameters $(H_0, \Omega_m, \Omega_\lambda) = (70\ {\rm km\ s^{-1}\ Mpc^{-1}}, 0.3, 0.7)$ (Spergel et al. 2003) are adopted throughout the Letter.

2. THE *SUZAKU* OBSERVATIONS AND RESULTS

Table 1 summarizes our targets and observation log. SWIFT J0601.9−8636 is optically identified as the galaxy ESO 005-G004 (Lauberts 1982) at $z = 0.0062$ with no previous firm evidence for AGN activity. The optical counterpart of SWIFT J0138.6−4001 is the galaxy ESO 297-G018 (Lauberts 1982) at $z = 0.0252$, which was identified as a narrow-line AGN (Kirhakos & Steiner 1990).

Suzaku, the fifth Japanese X-ray satellite, carries four sets of X-ray mirrors, each with a focal plane X-ray CCD camera, the X-ray Imaging Spectrometer (XIS-0, XIS-1, XIS-2, and XIS-3; Koyama et al. 2007), and a nonimaging instrument called the Hard X-ray Detector (HXD; Takahashi et al. 2007), which consists of the Si PIN photodiodes and GSO scintillation counters. The XIS and PIN simultaneously cover the energy bands of 0.2–12 and 10–70 keV, respectively. The unique capabilities of *Suzaku*, high sensitivity in the 12–70 keV band and broadband coverage with good spectral resolution, are critical for studies of highly absorbed AGNs.

We observed SWIFT J0601.9−8636 and SWIFT J0138.6−4001 with *Suzaku* on 2006 April 14 and June 5 for a net exposure of 20 and 21 ks (for the XIS), respectively. Standard analysis was made on data products, which were processed with the latest calibration (ver. 1.2). We detected both sources at high significance

[1] Department of Astronomy, Kyoto University, Kyoto 606-8502, Japan.
[2] Department of Physics, Faculty of Science, Ehime University, Matsuyama 790-8577, Japan.
[3] NASA Goddard Space Flight Center, Greenbelt, MD 20771.
[4] South African Astronomical Observatory, Observatory 7935, South Africa.

TABLE 1
TARGETS AND OBSERVATION LOG

SWIFT	Optical Identification	Redshift	Start Time (UT)	End Time	Exposure[a] (ks)
J0601.9−8636	ESO 005-G004	0.0062	2006 Apr 13 16:24	Apr 14 01:52	19.8
J0138.6−4001	ESO 297-G018	0.0252	2006 Jun 04 18:13	Jun 05 05:00	21.2

[a] Based on a good time interval for the XIS-0.

with the XIS and PIN. The XIS spectra were accumulated within a radius of 2′ around the detected position. The background was taken from a source-free region in the field of view. The spectra of three front-side illuminated CCDs (FI-XIS; XIS-0, 2, and 3) are summed together, while that of the back-side illuminated CCD (BI-XIS; XIS-1) is treated separately in the spectral fit. Examining the spectra of the ^{55}Fe calibration source, we verify that the energy scale and resolution is accurate better than 10 and 60 eV levels, respectively, at 5.9 keV. For the analysis of the PIN, we utilized only data of Well units with the bias voltage set at 500 eV (W0, 1, 2, 3 for SWIFT J0601.9−8636 and W1, 2, 3 for SWIFT J0138.6−4001) with the best available models of PIN background provided by the HXD team.[5]

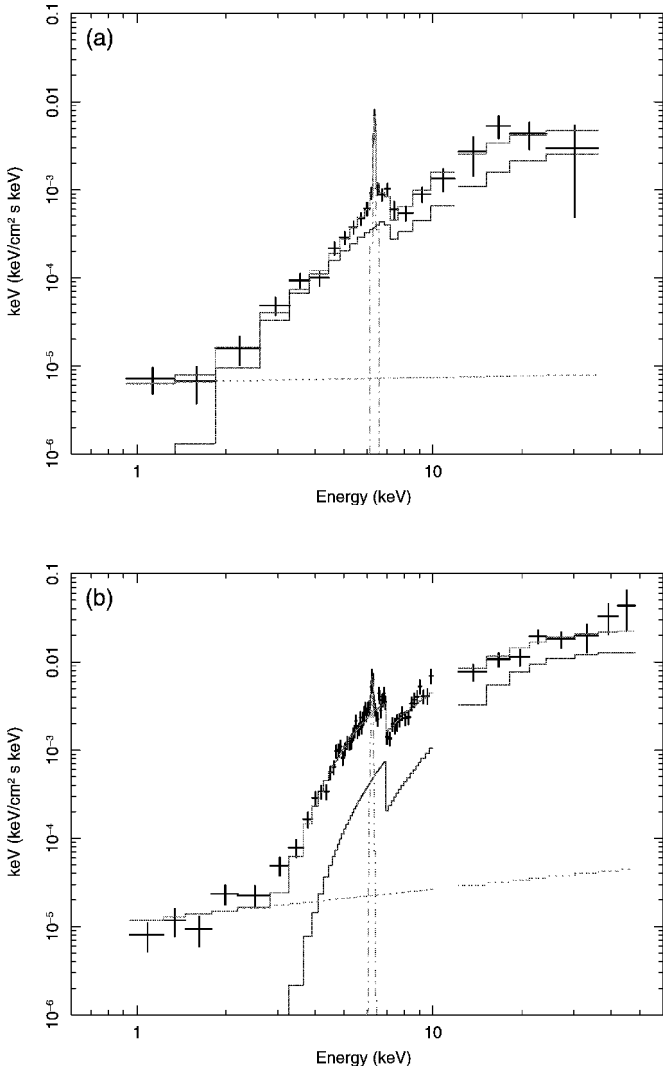

FIG. 1.—Broadband energy spectra of (*a*) SWIFT J0601.9−8636 and (*b*) SWIFT J0138.6−4001 unfolded for the detector response in units of $E^2F(E)$, where $F(E)$ is the photon spectrum. For clarity, we only plot the summed spectrum of the three FI-XIS (below 12 keV), and those of PIN (above 12 keV), while the spectral fit is performed to the whole XIS+PIN+BAT data including the BI-XIS. The black crosses represent the data with 1 σ statistical errors. The histograms show the best-fit model with separate components. The upper solid line, dot-dashed line, lower solid line, and dotted line correspond to the total, iron K emission line, reflection component, and scattered component, respectively. [*See the electronic edition of the Journal for a color version of this figure.*]

To obtain the best constraint from the entire data, we perform a simultaneous fit to the spectra of XIS (FI and BI), PIN, and the archival *Swift* BAT, which covers the 0.2–200 keV band as a whole. The BAT spectra consist of four energy bins over the 15–200 keV range and are useful to constrain the power-law index. Here we allow the relative flux normalization between *Suzaku* and *Swift* (BAT) to be a free parameter, considering possible time variability between the observations. We fixed the normalization ratio between the FI-XIS and the PIN based on the calibration result using the Crab Nebula. All the absolute fluxes quoted in this Letter refer to the flux calibration of the FI-XIS. We find that the 10–50 keV PIN fluxes of SWIFT J0601.9−8636 and SWIFT J0138.6−4001 are 1×10^{-11} and 4×10^{-11} ergs cm^{-2} s^{-1}, indicating time variability by a factor of 0.5 and 1.6, respectively, compared with the averaged flux measured by the *Swift* BAT over the past 9 months (J. Tueller et al. 2007, in preparation).

Figure 1 shows the FI-XIS and PIN spectra unfolded for the detector response (for clarity, the BI-XIS and BAT spectra are not plotted). The X-ray spectrum of SWIFT J0601.9−8636 below 10 keV is dominated by a hard continuum with few photons below 2 keV, consistent with the previous nondetection in soft X-rays (an upper limit of 1.3×10^{-13} ergs cm^{-2} s^{-1} in the 0.1–2.4 keV band by the *ROSAT* All Sky Survey; Voges et al. 2000). We find that the broadband spectrum can be well reproduced with a model consisting of a heavily absorbed power law with $\log N_{\rm H} \simeq 24$ cm^{-2}, which dominates above 10 keV, and a mildly absorbed reflection component from cold matter accompanied by a narrow fluorescence iron K line, which dominates below 10 keV. The large column density is consistent with the observed equivalent width (EW) of the iron K line, ≈1 keV (Levenson et al. 2002). SWIFT J0138.6−4001 shows a similar spectrum but with a smaller absorption of $\log N_{\rm H} = 23.7$ cm^{-2} for both transmitted and reflected components.

The spectral model is represented as

$$F(E) = e^{-\sigma(E)N_{\rm H}^{\rm Gal}}[fAE^{-\Gamma} + e^{-\sigma(E)N_{\rm H}}AE^{-\Gamma} + e^{-\sigma(E)N_{\rm H}^{\rm refl}}C(E) + G(E)],$$

where $N_{\rm H}^{\rm Gal}$ is the Galactic absorption column density fixed at 2.0×10^{20} cm^{-2} for both targets (Dickey & Lockman 1990), $N_{\rm H}$ is the local absorption column density at the source redshift for the transmitted component, $N_{\rm H}^{\rm refl}$ is that for the reflected component (assumed to be the same as $N_{\rm H}$ for SWIFT J0138.6−4001), and $\sigma(E)$ is the cross section of photoelectric absorption. The term $C(E)$ represents the reflection component, calculated using the

[5] Ver1.2_d for SWIFT J0601.9−8636 and ver1.2_w123 for SWIFT J0138.6−4001.

TABLE 2
BEST-FIT SPECTRAL PARAMETERS

Parameter	SWIFT J0601.9−8636	SWIFT J0138.6−4001
N_H[a] (10^{22} cm^{-2})	101^{+54}_{-38}	46 ± 4
Γ[b]	$1.95^{+0.36}_{-0.33}$	$1.66^{+0.16}_{-0.04}$
R[c]	$1.7^{+3.5}_{-0.9}$	$2.1^{+0.4}_{-1.2}$
N_H^{refl}[d] (10^{22} cm^{-2})	$2.9^{+5.3}_{-1.4}$	$(=N_H)$
f_{scat}[e] (%)	0.20 ± 0.11	$0.23^{+0.23}_{-0.16}$
E_{cen}[f] (keV)	6.38 ± 0.02	6.38 ± 0.03
EW[g] (keV)	1.06 ± 0.16	0.20 ± 0.05
F_{2-10}[h] (ergs cm^{-2} s^{-1})	1.1×10^{-12}	3.3×10^{-12}
F_{10-50}[i] (ergs cm^{-2} s^{-1})	9.8×10^{-12}	3.9×10^{-11}
L_{2-10}[j] (ergs s^{-1})	8.3×10^{41}	3.9×10^{43}
χ^2 (dof)	20.0 (27)	101.3 (87)

[a] The line-of-sight hydrogen column density for the transmitted component.
[b] The power-law photon index.
[c] The relative strength of the reflection component to the transmitted one, defined as $R \equiv \Omega/2\pi$, where Ω is the solid angle of the reflector viewed from the nucleus.
[d] The line-of-sight hydrogen column density for the refection component (assumed to be the same as N_H for SWIFT J0138.6−4001).
[e] The fraction of a scattered component relative to the intrinsic power law corrected for the transmission efficiency of $1/R$ when $R > 1$.
[f] The center energy of an iron K emission line at rest frame. The 1 σ line width is fixed at 50 eV.
[g] The observed equivalent width of the iron K line with respect to the whole continuum.
[h] Observed fluxes in the 2–10 keV band.
[i] Observed fluxes in the 10–50 keV band.
[j] The 2–10 keV intrinsic luminosity corrected for the absorption and transmission efficiency of $1/R$. The errors are 90% confidence limits for a single parameter.

code in Magdziarz & Zdziarski (1995); we leave the solid angle Ω of the reflector as a free parameter by fixing the inclination angle at 60° and cutoff energy at 300 keV, assuming solar abundances for all elements; $R(\equiv \Omega/2\pi) > 1$ means the transmission efficiency should be $\lesssim 1/R$ (see § 4). The term $G(E)$ is the narrow iron K emission line modeled by a Gaussian profile, where we fix the 1 σ width at 50 eV to take account of the response uncertainty (and hence, the line should be considered to be unresolved). The best-fit parameters are summarized in Table 2 with the intrinsic 2–10 keV luminosity, L_{2-10}, corrected for the absorption and transmission efficiency of $1/R$.

We confirm that these results are robust, within the statistical error, given the systematic errors in the background estimation of the PIN detector (Kokubun et al. 2007). In the case of SWIFT J0138.6−4001, where photon statistics is dominated by the XIS data, we limit the allowed range of photon index to $\Gamma = 1.63$–2.02 in the simultaneous fit, being constrained from the BAT spectrum. We have limited $R < 2.5$ for this source to avoid physical inconsistency between R and the EW of an iron K line; otherwise (i.e., in more "reflection-dominated" spectra), we should expect a larger EW than the observed value of $\approx$0.2 keV.

3. OPTICAL SPECTRUM OF SWIFT J0601.9−8636

We performed an optical spectroscopic observation of SWIFT J0601.9−8636 (ESO 005-G004) during the night of 2007 March 16, using the SAAO 1.9 m telescope with the Cassegrain spectrograph. Grating six, with a spectral range of about 3500–5300 Å at a resolution around 4 Å, was used with a 2″ slit placed on the center of the galaxy for a total integration time of 2400 s. To derive the sensitivity curve, we fit the observed spectral energy distribution of standard stars with a low-order polynomial. The co-added, flux-calibrated spectrum in the 4000–5500 Å range is shown in Figure 2. It reveals a rather featureless spectrum with no evidence for Hβ or [O III] λ5007 emission lines, typical for this type of nonactive

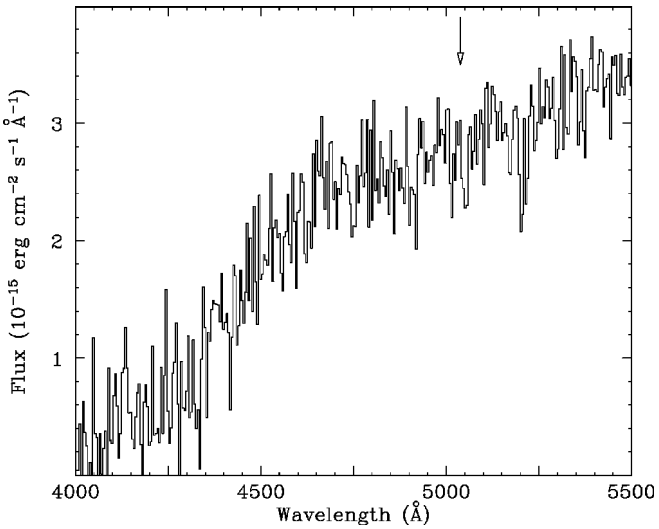

FIG. 2.—Optical spectrum of the nucleus region of SWIFT J0601.9−8636 (ESO 005-G004) in the 4000–5500 Å wavelength range, taken with the SAAO 1.9 m telescope. The arrow denotes the position of the [O III] λ5007 line.

edge-on galaxy within this spectral range. The 90% upper limit on the [O III] flux is conservatively estimated to be 3×10^{-15} ergs cm^{-2} s^{-1}, corresponding to a luminosity of 3×10^{38} ergs s^{-1}. This yields the ratio of the intrinsic 2–10 keV luminosity to the *observed* [O III] luminosity of >2800. Although the (unknown) extinction correction for [O III] could reduce the value, the result is consistent with SWIFT J0601.9−8636 having an intrinsically weak [O III] emission relative to hard X-rays compared with other Seyfert galaxies (Bassani et al. 1999; Heckman et al. 2005; Netzer et al. 2006). In particular, this object would not have been selected to be an AGN on the basis of its [O III] or Hβ emission.

4. DISCUSSION

Both sources show an intense reflection component relative to the transmitted one. Using the standard reflection model (Magdziarz & Zdziarski 1995), we find that the solid angle of the reflector $\Omega/2\pi$ viewed from the nucleus exceeds unity, which is apparently unphysical if attributed only to geometry. This implies that a part of the direct emission is completely blocked by nonuniform material in the line of sight even above 10 keV. The reflection-dominated nature of the spectra of heavily obscured AGNs, if common, has an impact on the population synthesis model of the XRB, where a much weaker reflection is assumed for type 2 AGNs (Gilli et al. 2007). Another possibility is that this apparent very high reflection fraction is due to time variability, that is, the decrease of the flux in the transmitted light is echoed with a time delay corresponding to the difference in light paths between the emitter, reflector, and observers.

It is remarkable that both SWIFT J0601.9−8636 and SWIFT J0138.6−4001 have a very small amount of soft X-ray scattered emission, less than 0.46% of the intrinsic power-law component. (If we fix $N_H^{refl} = 0$ in the spectral fit of SWIFT J0601.9−8636, then we obtain a photon index of 1.80 ± 0.29 and no significant scattered component with a 90% upper limit of 0.47%.) As far as we know, these are among the lowest scattered fractions ever seen from an absorbed AGN (Turner et al. 1997; Cappi et al. 2006). In optically selected Seyfert 2 galaxies, the presence of prominent soft X-ray emission is common (e.g., Guainazzi et al. 2005). Such emission probably originates from the same extended gas responsible for the optical [O III] emission (Bianchi et al. 2006). This type of emission from "classical" Seyfert 2

galaxies has always been seen in the spectra of objects well studied so far. However, this sample is dominated by optically selected Seyfert 2 galaxies, which require a scattered component to be selected.

The scattered fraction is proportional to both the solid angle of the scattering region as viewed from the nucleus, $\Omega_{\rm scat}$, and the scattering optical depth, $\tau_{\rm scat}$. Hence, the observed small scattered fraction means small $\Omega_{\rm scat}$ and/or small $\tau_{\rm scat}$, i.e., deficiency of gas in the circumnuclear environment, for some unknown reason.

The first possibility, which we favor as a more plausible case, indicates that these AGNs are buried in a very geometrically thick obscuring torus. Assuming that the typical scattering fraction of 3% corresponds to the effective torus half-opening angle (see Levenson et al. 2002 for definition) θ of 45°, our results (<0.5%) indicate $\theta \lesssim 20°$. In the case of SWIFT J0601.9−8636, the small absorption for the reflection component, which probably comes from the inner wall of the torus, suggests that we are seeing this source in a rather face-on geometry. Indeed, applying the formalism of Levenson et al. (2002) to the observed EW of the iron K line, we infer that the inclination angle with respect to the axis of the disk, i, is smaller than 40° if $\theta < 20°$. For SWIFT J0138.6−4001, the presence of a high column density for the reflection component implies a more edge-on geometry than in SWIFT J0601.9−8636. The observed EW of 0.20 ± 0.05 keV can be explained if the torus is patchy or has a geometrical structure such that the line-of-sight column density is much smaller than that in the disk plane.

We infer that this type of buried AGN is a significant fraction of the whole AGN population, although an accurate estimate of this fraction is difficult at present due to the small number statistics.[6] The observed fraction of heavily obscured AGNs with $\log N_{\rm H} > 23.5$ is about 25% among the hard X-ray ($E > 15$ keV) selected AGNs (Markwardt et al. 2005). The true number density of obscured AGNs could be much larger, however. If we saw the same system of our targets at much larger inclination angles ($i \gg 40°$), the observed flux of the transmitted component would be much fainter even in hard X-rays due to the effects of repeated Compton scatterings (Wilman & Fabian 1999). Our results imply that there must be a large number of yet unrecognized, Compton thick AGNs in the local universe, which are likely to be missed even in the *Swift* and *INTEGRAL* surveys.

[6] We note that a similar object has also been found by Comastri et al. (2007) with the *Suzaku* follow-up of hard X-ray (>10 keV) selected AGNs.

The existence of AGNs with a geometrically thick torus was predicted by Fabian et al. (1998), where the extreme obscuration was postulated to be caused by a nuclear starburst. Using the 60 and 100 μm fluxes measured by the *Infrared Astronomical Satellite*, we obtain the far-infrared luminosity (defined by David et al. 1992) of $L_{\rm FIR} = 4.4 \times 10^{43}$ and 7.1×10^{43} ergs s^{-1}, and hence the ratio of the 2–10 keV to far-infrared luminosities of $L_{2-10}/L_{\rm FIR} \approx 0.02$ and $\approx$0.5 for SWIFT J0601.9−8636 and SWIFT J0138.6−4001, respectively. While the result of SWIFT J0138.6−4001 is consistent with those of the 2–10 keV selected AGNs in the local universe (Piccinotti et al. 1982) within the scatter, the small $L_{2-10}/L_{\rm FIR}$ ratio of SWIFT J0601.9−8636 indicates possibly significant starburst activity. However, this is not supported by the optical spectrum of this object, which apparently shows no evidence for a significant amount of star formation. The reason behind the difference between the two sources is unclear.

By using the unique combination of the *Swift* BAT survey and the *Suzaku* broadband spectral capabilities, we are discovering a new type of AGN with an extremely small scattering fraction. This class of object is most likely to contain a buried AGN in a very geometrically thick torus. This population was missed in previous surveys, demonstrating the power of hard X-ray (>10 keV) surveys to advance our global understanding of the whole AGN population. In particular, we predict that the objects should have fainter [O III] emission luminosity relative to the hard X-ray luminosity compared with classical Seyfert 2 galaxies because much less of the nuclear flux "leaks" out to ionize the narrow-line gas. As shown above, the optical spectrum of SWIFT J0601.9−8636 is consistent with this prediction. This study is particularly important since the existence of numerous such objects would make surveys that rely on the [O III] emission incomplete by missing many buried AGNs and incorrectly estimating the true AGN luminosity.

We thank the members of the *Suzaku* team for calibration efforts of the instruments, in particular Motohide Kokubun and Yasushi Fukazawa for their useful advice regarding the background of the HXD. We would also like to thank the anonymous referee for providing helpful suggestions to improve this Letter. Part of this work was financially supported by Grants-in-Aid for Scientific Research 17740121 and 17740124, and by the Grant-in-Aid for the 21st Century COE "Center for Diversity and Universality in Physics" from the Ministry of Education, Culture, Sports, Science, and Technology (MEXT) of Japan.

REFERENCES

Bassani, L., et al. 1999, ApJS, 121, 473
———. 2006, ApJ, 636, L65
Beckmann, V., Gehrels, N., Shrader, C. R., & Soldi, S. 2006, ApJ, 638, 642
Bianchi, S., Guainazzi, M., & Chiaberge, M. 2006, A&A, 448, 499
Cappi, M., et al. 2006, A&A, 446, 459
Comastri, A., Gilli, R., Vignali, C., Matt, G., Fiore, F., & Iwasawa, K. 2007, Prog. Theor. Phys. Suppl., in press (arXiv: 0704.1253)
David, L. P., Jones, C., & Forman, W. 1992, ApJ, 388, 82
Dickey, J. M., & Lockman, F. J. 1990, ARA&A, 28, 215
Fabian, A. C. 1999, MNRAS, 308, L39
Fabian, A. C., Barcons, X., Almaini, O., & Iwasawa, K. 1998, MNRAS, 297, L11
Gilli, R., Comastri, A., & Hasinger, G. 2007, A&A, 463, 79
Guainazzi, M., Matt, G., & Perola, G. C. 2005, A&A, 444, 119
Heckman, T. M., Ptak, A., Hornschemeier, A., & Kauffmann, G. 2005, ApJ, 634, 161
Kirhakos, S. D., & Steiner, J. E. 1990, AJ, 99, 1722
Kokubun, M., et al. 2007, PASJ, 59, S53
Koyama, K., et al. 2007, PASJ, 59, S23
Lauberts, A. 1982, ESO/Uppsala Survey of the ESO(B) Atlas (Garching: ESO)
Levenson, N. A., Krolik, J. H., Zycki, P. T., Heckman, T. M., Weaver, K. A., Awaki, H., & Terashima, Y. 2002, ApJ, 573, L81
Magdziarz, P., & Zdziarski, A. A. 1995, MNRAS, 273, 837
Maiolino, R., et al. 1998, A&A, 338, 781
Marconi, A., Risaliti, G., Gilli, R., Hunt, L. K., Maiolino, R., & Salvati, M. 2004, MNRAS, 351, 169
Markwardt, C. B., Tueller, J., Skinner, G. K., Gehrels, N., Barthelmy, S. D., & Mushotzky, R. F. 2005, ApJ, 633, L77
Mitsuda, K., et al. 2007, PASJ, 59, S1
Netzer, H., Mainieri, V., Rosati, P., & Trakhtenbrot, B. 2006, A&A, 453, 525
Piccinotti, G., Mushotzky, R. F., Boldt, E. A., Holt, S. S., Marshall, F. E., Serlemitsos, P. J., & Shafer, R. A. 1982, ApJ, 253, 485
Risaliti, G., Maiolino, R., & Salvati, M. 1999, ApJ, 522, 157
Sazonov, S., Revnivtsev, M., Krivonos, R., Churazov, E., & Sunyaev, R. 2007, A&A, 462, 57
Setti, G., & Woltjer, L. 1989, A&A, 224, L21
Spergel, D. N., et al. 2003, ApJS, 148, 175
Takahashi, T., et al. 2007, PASJ, 59, S35
Turner, T. J., George, I. M., Nandra, K., & Mushotzky, R. F. 1997, ApJS, 113, 23
Ueda, Y., Akiyama, M., Ohta, K., & Miyaji, T. 2003, ApJ, 598, 886
Voges, W., et al. 2000, IAU Circ., 7432, 3
Wilman, R. J., & Fabian, A. C. 1999, MNRAS, 309, 862